

# **Ionic Liquid Electrolytes for Flexible Dye-Sensitized Solar Cells**

**by Charles Brandon Sweeney, Mark Bundy, Mark Griep, and  
Shashi P. Karna**

**ARL-TR-7100**

**September 2014**

## **NOTICES**

### **Disclaimers**

The findings in this report are not to be construed as an official Department of the Army position unless so designated by other authorized documents.

Citation of manufacturer's or trade names does not constitute an official endorsement or approval of the use thereof.

Destroy this report when it is no longer needed. Do not return it to the originator.

# **Army Research Laboratory**

Aberdeen Proving Ground, MD 21005-5069

---

**ARL-TR-7100****September 2014**

---

## **Ionic Liquid Electrolytes for Flexible Dye-Sensitized Solar Cells**

**Charles Brandon Sweeney**  
**Texas A&M University**

**Mark Bundy**  
**Vehicle Technology Directorate, ARL**

**Mark Griep and Shashi P. Karna**  
**Weapons and Material Research Directorate, ARL**

REPORT DOCUMENTATION PAGE				Form Approved OMB No. 0704-0188	
Public reporting burden for this collection of information is estimated to average 1 hour per response, including the time for reviewing instructions, searching existing data sources, gathering and maintaining the data needed, and completing and reviewing the collection information. Send comments regarding this burden estimate or any other aspect of this collection of information, including suggestions for reducing the burden, to Department of Defense, Washington Headquarters Services, Directorate for Information Operations and Reports (0704-0188), 1215 Jefferson Davis Highway, Suite 1204, Arlington, VA 22202-4302. Respondents should be aware that notwithstanding any other provision of law, no person shall be subject to any penalty for failing to comply with a collection of information if it does not display a currently valid OMB control number. <b>PLEASE DO NOT RETURN YOUR FORM TO THE ABOVE ADDRESS.</b>					
1. REPORT DATE (DD-MM-YYYY) September 2014		2. REPORT TYPE Final		3. DATES COVERED (From - To) June 2012–August 2013	
4. TITLE AND SUBTITLE Ionic Liquid Electrolytes for Flexible Dye-Sensitized Solar Cells				5a. CONTRACT NUMBER	
				5b. GRANT NUMBER	
				5c. PROGRAM ELEMENT NUMBER	
6. AUTHOR(S) Charles Brandon Sweeney, Mark Bundy, Mark Griep, and Shashi P. Karna				5d. PROJECT NUMBER	
				5e. TASK NUMBER	
				5f. WORK UNIT NUMBER	
7. PERFORMING ORGANIZATION NAME(S) AND ADDRESS(ES) U.S. Army Research Laboratory ATTN: RDRL-VTM Aberdeen Proving Ground, MD 21005-5069				8. PERFORMING ORGANIZATION REPORT NUMBER ARL-TR-7100	
9. SPONSORING/MONITORING AGENCY NAME(S) AND ADDRESS(ES)				10. SPONSOR/MONITOR'S ACRONYM(S)	
				11. SPONSOR/MONITOR'S REPORT NUMBER(S)	
12. DISTRIBUTION/AVAILABILITY STATEMENT Approved for public release; distribution is unlimited.					
13. SUPPLEMENTARY NOTES					
14. ABSTRACT In developing multifunctional robotic platforms, there has been an increasing need to extend the effective runtime of these units to give them more practical battlefield applications. Therefore, robust power solutions, which may be incorporated into any structural system, need to be realized. Solar energy is an abundant renewable resource capable of meeting the power requirements for a wide range of robotic vehicles. Dye-sensitized solar cells (DSSCs) have recently become a competitive photovoltaic technology due to their low manufacturing cost and relatively high efficiency. However, the liquid electrolyte commonly employed in DSSCs limits the potential for flexible cells manufactured using reel-to-reel printing methods. Furthermore, these liquid electrolytes must be hermetically sealed to operate properly and prevent off-gassing of volatile organic compounds. Herein we present a study of nonvolatile room temperature ionic liquid electrolytes and their resulting performance in flexible DSSCs.					
15. SUBJECT TERMS dye-sensitized solar cells, RTIL electrolyte, flexible, photovoltaic, energy harvesting					
16. SECURITY CLASSIFICATION OF:			17. LIMITATION OF ABSTRACT  UU	18. NUMBER OF PAGES  20	19a. NAME OF RESPONSIBLE PERSON Mark Bundy
a. REPORT Unclassified	b. ABSTRACT Unclassified	c. THIS PAGE Unclassified			19b. TELEPHONE NUMBER (Include area code) 410-278-4318

---

## Contents

---

<b>List of Figures</b>	<b>iv</b>
<b>List of Tables</b>	<b>v</b>
<b>Acknowledgments</b>	<b>vi</b>
<b>1. Introduction and Background</b>	<b>1</b>
<b>2. Experiment and Calculations</b>	<b>2</b>
2.1 Materials .....	2
2.2 Test Cell Construction.....	3
2.3 Electrolyte Synthesis .....	4
2.4 Low Temperature TiO <sub>2</sub> Paste .....	4
<b>3. Results and Discussion</b>	<b>5</b>
<b>4. Summary and Conclusion</b>	<b>10</b>
<b>5. References</b>	<b>11</b>
<b>Distribution List</b>	<b>12</b>

---

## List of Figures

---

Figure 1. (A) Diagram of the operation of a dye-sensitized solar cell. (B) Electrodynamics of an operating dye-sensitized solar cell. The sensitizing dye excites an electron from the HOMO (D) (highest occupied molecular orbital) to the LUMO (D*) (lowest unoccupied molecular orbital) band where it is injected into the mesoporous $\text{TiO}_2$ conduction band to drive an external load. The cycle is complete when the electrons reduce the electrolyte at the platinum counter electrode converting triiodide back to iodide ions, which diffuse back towards the dye molecules to regenerate them. ....	1
Figure 2. Diagram of test cell construction, consisting of an ITO glass slide with a dye-loaded mesoporous film, covered with a platinized ITO counter-electrode. ....	4
Figure 3. Absolute irradiance spectrum of the Newport solar simulator recorded with a Jaz spectrophotometer manufactured by Ocean Optics. Notable peaks shown are 470, 765, 824, and 884 nm. ....	5
Figure 4. Current vs. voltage plot for the three different low-temperature sintering electrodes (prepared in a co-sensitizer dye mix and employing EL-HPE electrolyte). The area of the test cell photoanode for each device was $1\text{cm}^2$ . ....	6
Figure 5. UV-Vis spectra of dyes D149, N719, and a 1:1 mixture. ....	7
Figure 6. Current-voltage plots of DSSC test cells made with commercial Dyesol paste and dyes N719, D149, and an equimolar mix of the two. ....	8
Figure 7. Current density vs. voltage plot for the nonvolatile RTIL electrolytes B136 (circle markers) and Z132 (triangle markers). Also shown is the max power rectangle inscribed and fill factor of the cells. ....	9

---

## List of Tables

---

Table 1. Results of the tested electrolyte systems in standard test cells. ....	9
---	---

---

## **Acknowledgments**

---

The author would like to thank Dr. Mark Bundy and Dr. Mark Griep for mentoring him in this project. Special thanks to Dr. Shashi Karna for lab assistance and technical advice. The author is grateful to the U.S. Army Research Laboratory for providing the facilities and resources to complete this research. Finally, this project was made possible by Oak Ridge Institute for Science and Education/Oak Ridge Associated Universities funding for the summer research period.



# 1. Introduction and Background

Solar energy is an abundant renewable resource suitable for providing the power demands of many electronic devices. To harvest this radiant energy and convert it into useful electric current, a photovoltaic device is implemented, typically consisting of a p-n junction fabricated from doped semiconductors such as silicon. Many photovoltaic technologies have been developed since the advent of semiconductor processing, yet few systems boast cost-effective lightweight flexible designs, adept to mass-manufacturing methods. One technology poised to meet these demands is called a dye-sensitized solar cell (DSSC), invented by Michael Grätzel and Brian O'Regan in 1991 (1).

As described in their original *Nature* paper "A Low-Cost, High-Efficiency Solar-Cell Based on Dye-Sensitized Colloidal TiO<sub>2</sub> Films," a DSSC consists of four main components: a photoanode, a counter-electrode, a dye, and an electrolyte. Figure 1 shows the operation of the cell, where dye molecules adsorbed onto the TiO<sub>2</sub> (titanium dioxide) nanoparticles absorb incident photons with energy ( $h\nu$ ), and inject a photoelectron into the conduction band of the titanium dioxide (2). Simultaneously, a hole is created locally on the oxidized dye molecule where it will either interact with an iodide molecule in the electrolyte reducing the oxidized dye back to the photoactive state, or recombine with an electron in the TiO<sub>2</sub>. After donating two electrons to the dye molecules, the iodide ions oxidize to form a triiodide ion, which diffuses back to the platinum or carbon counter-electrode to be reduced; this cycle is repeated throughout the life of the cell.

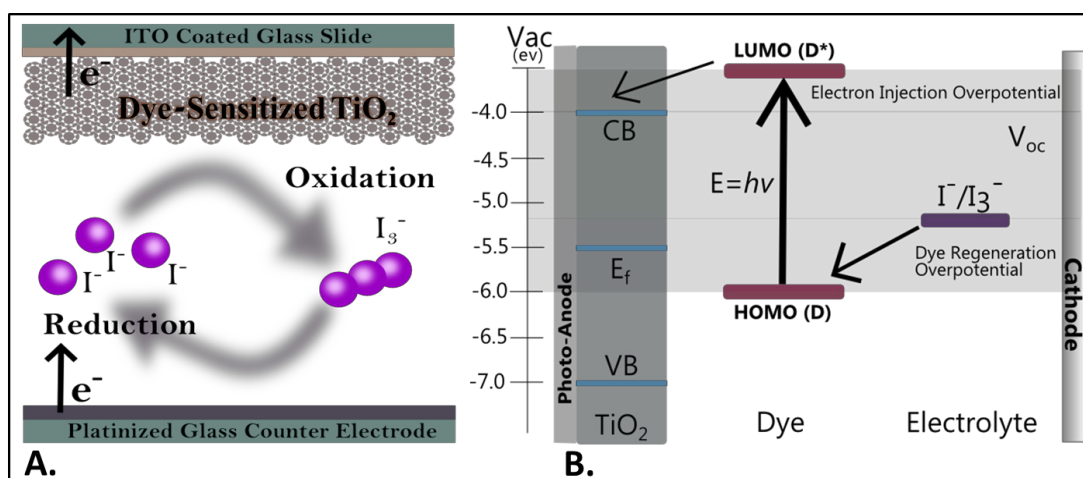


Figure 1. (A) Diagram of the operation of a dye-sensitized solar cell. (B) Electrodynamics of an operating dye-sensitized solar cell. The sensitizing dye excites an electron from the HOMO (D) (highest occupied molecular orbital) to the LUMO (D\*) (lowest unoccupied molecular orbital) band where it is injected into the mesoporous TiO<sub>2</sub> conduction band to drive an external load. The cycle is complete when the electrons reduce the electrolyte at the platinum counter electrode converting triiodide back to iodide ions, which diffuse back towards the dye molecules to regenerate them.

The dye usually consists of a metal complex such as a ruthenium bipyridine, excited by a metal-to-ligand charge transfer, or an organic compound such as an indoline or anthocyanin molecule excited by a donor- $\pi$ -acceptor transition (3). These dye molecules attach to the titania nanoparticles via carboxylate groups which also help channel excited electrons into the  $\text{TiO}_2$  conduction band (4).

Typical electrolytes for DSSC's consist of an iodide/triiodide redox pair dissolved in a suitable organic solvent such as acetonitrile. The use of volatile organic solvents is, however, an issue for the commercial production of DSSCs, requiring that the cells be hermetically sealed against leakage to prevent the electrolyte from evaporating out of the device causing failure (5).

Furthermore, many of the organic compounds used in these electrolyte systems are hazardous to human health and the environment, thus it is desirable to replace volatile organic solvents with more eco-friendly room temperature ionic liquids (RTILs).

RTILs consist of bulky anion and cation pairs that do not easily crystallize at room temperature due to steric hindrances (6). Because of this, many ionic liquids operate over a wide range of temperatures with little effect on their electrochemical properties. Ionic liquids generally have a negligible vapor pressure which mitigates the need for sealing the cells against evaporation and off-gassing. It has been reported in literature that blends of ionic liquids could provide improved performance as electrolytes in DSSCs due to increased mismatch between ions, which reduces viscosity and electrochemical resistance of the blend (7). Here we report the characterization of different ionic liquid blends well suited for the fabrication of flexible solar cell modules.

---

## 2. Experiment and Calculations

---

### 2.1 Materials

Commercial  $\text{TiO}_2$  paste was purchased from Dyesol, and additional nanophase  $\text{TiO}_2$  powder for low temperature sintering experiments was supplied from Sigma Aldrich. Commercial electrolyte EL-HPE was purchased from Dyesol and used as-is for baseline characterization of DSSC test modules. Both the N719 ruthenium dye and D149 indoline-based organic dye were purchased from Sigma Aldrich and used without further purification. Additionally, lab-prepared electrolyte materials consisted of 1-butyl-3-methylimidazolium tetrafluoroborate (BMIm  $[\text{BF}_4]$ ), 1-butyl-3-methylimidazolium iodide (BMImI), lithium iodide, iodine, 1-N-methylbenzimidazole (NMBI), and guanidinium thiocyanate (GuanSCN), all purchased from Sigma Aldrich.

## 2.2 Test Cell Construction

The test cells were constructed on indium-tin oxide (ITO)-coated glass slides, and ITO-sputtered polyethylene terephthalate (PET Melinex<sup>1</sup> ST504) plastic substrates for the flexible cells. The ITO serves as a transparent conductive oxide, collecting charge carriers from the photoanode and cathode, to shuttle current into the silver ink contacts applied to the edges of each electrode. In fabricating the photoanode, about 1 mL of TiO<sub>2</sub> paste was applied to the ITO glass slide and spread on with a doctor blade technique to achieve a uniform film thickness. This slide was then sintered at 450 °C for an hour (120 °C for the plastic substrates) to remove binders in the TiO<sub>2</sub> paste and to promote electrical contact between the titania nanoparticles. While the slide was still hot at 80 °C, it was removed from the oven and placed directly in the co-sensitizer dye bath. The dye solutions prepared previously consist of 0.3-mM solutions of the N719 ruthenium and the D149 indoline dye, each dispersed in ethanol. The slide was left in the dye bath for 24 h to allow a monolayer of dye to adsorb onto the surface of the titania nanoparticles. After 24 h, the dye-sensitized titania slide was removed from the dye bath and rinsed with ethanol to remove unadsorbed dye. The counter-electrode was prepared by applying a catalytic platinum thin film of Platisol T/SP (Solaronix) to an ITO slide and firing at 450 °C for 15 min.

Current-collecting contacts consisting of conductive silver ink were applied to the edges of both the photoanode and counter-electrode and baked at 100 °C to remove solvents and fuse the ink to the ITO film. Finally, the two slides were brought face to face and fastened together with binder clips; electrolyte solution was introduced to the cell by applying one or two drops to the interface of the slides and allowing capillary action to draw the liquid into the TiO<sub>2</sub> mesopores. A diagram of the cell construction can be seen in figure 2.

---

<sup>1</sup>PET Melinex is a trademark of DuPont, Wilmington, DE.

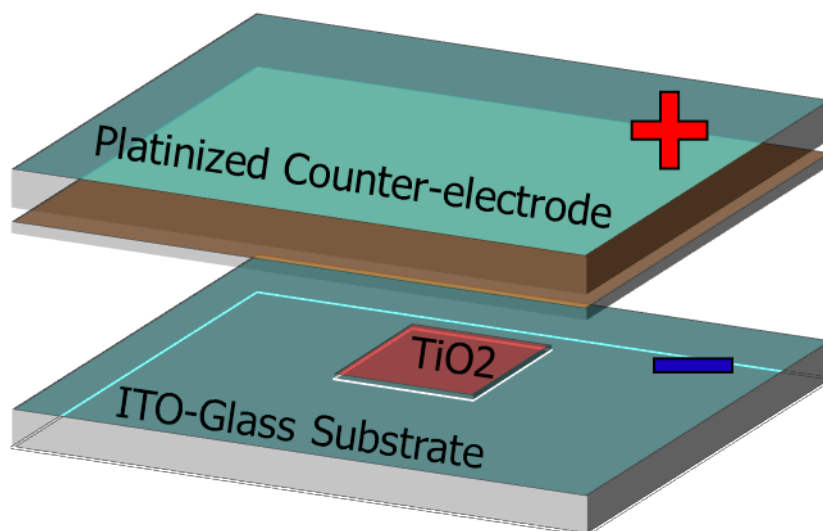


Figure 2. Diagram of test cell construction, consisting of an ITO glass slide with a dye-loaded mesoporous film, covered with a platinized ITO counter-electrode.

### 2.3 Electrolyte Synthesis

Several different electrolyte systems were investigated in this report, with an emphasis on moving toward ionic liquid electrolytes containing an iodide anion to participate in the redox reaction. One commercial electrolyte EL-HPE (Dyesol) was purchased and tested as a baseline measurement to compare the properties of the lab-prepared ionic liquid electrolytes. For the RTIL electrolytes, a high-viscosity and low-viscosity blend were characterized. The low-viscosity electrolyte, hereafter referred to as electrolyte B136, consisted of 0.6 M BMImI, 0.05 M I<sub>2</sub>, 0.1 M LiI, and 0.5 M *t*BP in MPN. The high-viscosity electrolyte termed Z132 consisted of 0.2 M I<sub>2</sub>, 0.2 M LiI, 0.1 M GuanSCN, and 0.5 M NMBI, in 25 mL BMIm[BF<sub>4</sub>] as a RTIL solvent. Each RTIL electrolyte was stirred at 70 °C for 24 h to ensure thorough mixing of the crystalline components.

### 2.4 Low Temperature TiO<sub>2</sub> Paste

The goal of this research was to develop electrolytes for flexible DSSCs deposited on plastic substrates. Techniques involving temperatures below the characteristic stability temperature (150 °C) of the PET film were investigated for use in constructing DSSC test cells. Each paste was applied to an ITO glass slide with a doctor blade and subsequently sintered at 120 °C for an hour. Glass was used in electrical characterization of the low-temperature pastes due to ease of cell construction for consistent measurements. Later, ITO-sputtered plastic substrates were implemented to evaluate the device performance on a flexible substrate.

In determining an optimal TiO<sub>2</sub> paste for low-sintering temperatures on the plastic substrate, three different blends of titania were used—two of which were mixed in the lab. A commercially purchased low-temperature sintering paste, Nanoxide DL from Solaronix, was used as an experimental control. The first lab-prepared paste consisted of 3.5 g Degussa P-25 TiO<sub>2</sub> nanoparticles mixed in 15 mL ethanol, to which 0.5 mL titanium isopropoxide was added. The entire mixture was then stirred for an hour followed, by 10 min of bath sonicating. The titanium isopropoxide is added to the paste to serve as a sol-gel cross-linking agent increasing the viscosity and stability of the applied paste (8). The other paste consisted of 1 g P-25 titania dispersed in 4.2 mL ethanol with 1.4-mL HCl (37%) added to increase the hydrodynamic radius of the titania nanoparticles; this in turn increases the viscosity of the paste (9).

---

### 3. Results and Discussion

---

The DSSCs were tested under 140-mW/cm<sup>2</sup> AM0 irradiation with a Newport solar simulator fitted with a Xe bulb and fiber-optic light guide fixture. The absolute spectral irradiance and power output of the solar simulator was captured with a Jaz (Ocean Optics) spectrometer as seen in figure 3; this plot is in accordance with literature-reported spectral outputs for corresponding Xe illumination sources.

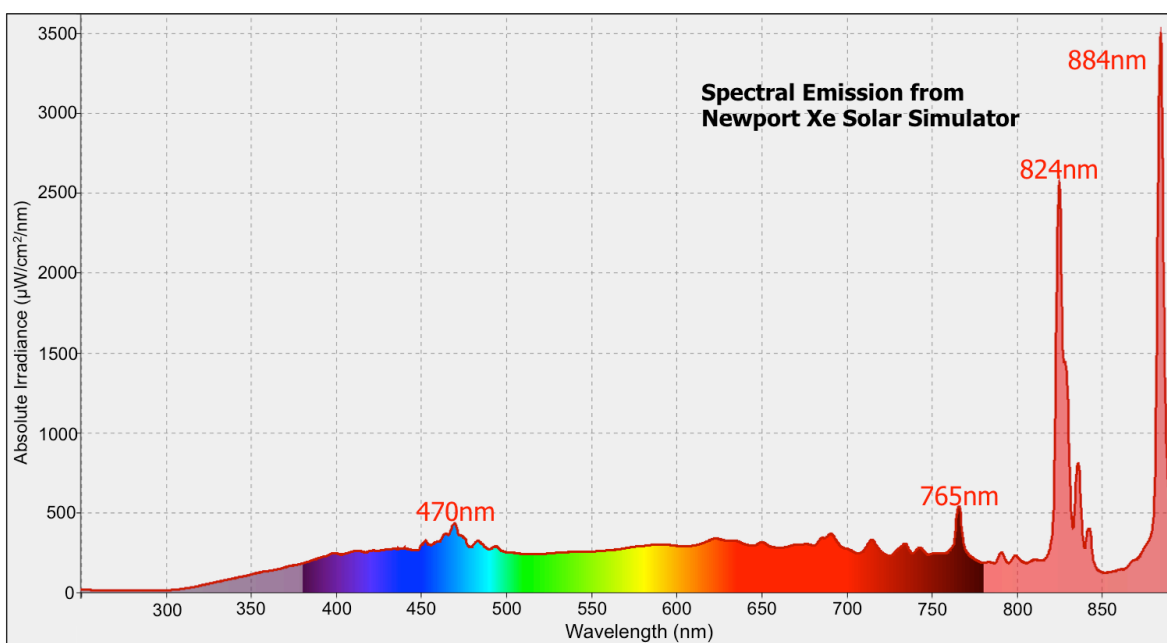


Figure 3. Absolute irradiance spectrum of the Newport solar simulator recorded with a Jaz spectrophotometer manufactured by Ocean Optics. Notable peaks shown are 470, 765, 824, and 884 nm.

The current-voltage sweeps were conducted with a Keithley 6430 Sub-Femtoamp Remote Source Meter and Labview program. A voltage sweep from 0.00 to 0.70 V, while sensing current, was conducted to determine both the maximum power output and theoretical power output. The fill factor may be calculated by multiplying the open circuit voltage  $V_{oc}$  by the short circuit current density  $J_{sc}$  and dividing by the maximum power on the I-V curve. A test cell, as described in section 2.2, was fabricated with each type of low-temperature  $TiO_2$  paste and JV sweeps were run to determine which cell produced the most power. The resultant plots of DSSC test cells for determining the optimal low-temperature paste can be seen in figure 4. The paste does not affect the electrochemistry or material energy levels, so the  $V_{oc}$  stays relatively constant while the photocurrent changes with each sample, indicating better interparticle contact. This implies that less recombination is occurring at each nanoparticle so the overall short circuit current density increases. The titania paste incorporating the HCl to improve viscosity performed the best, having a short circuit current density  $J_{sc}$  of about  $9 \text{ mA cm}^{-2}$ , thus it was selected as the baseline paste for future cell characterization.

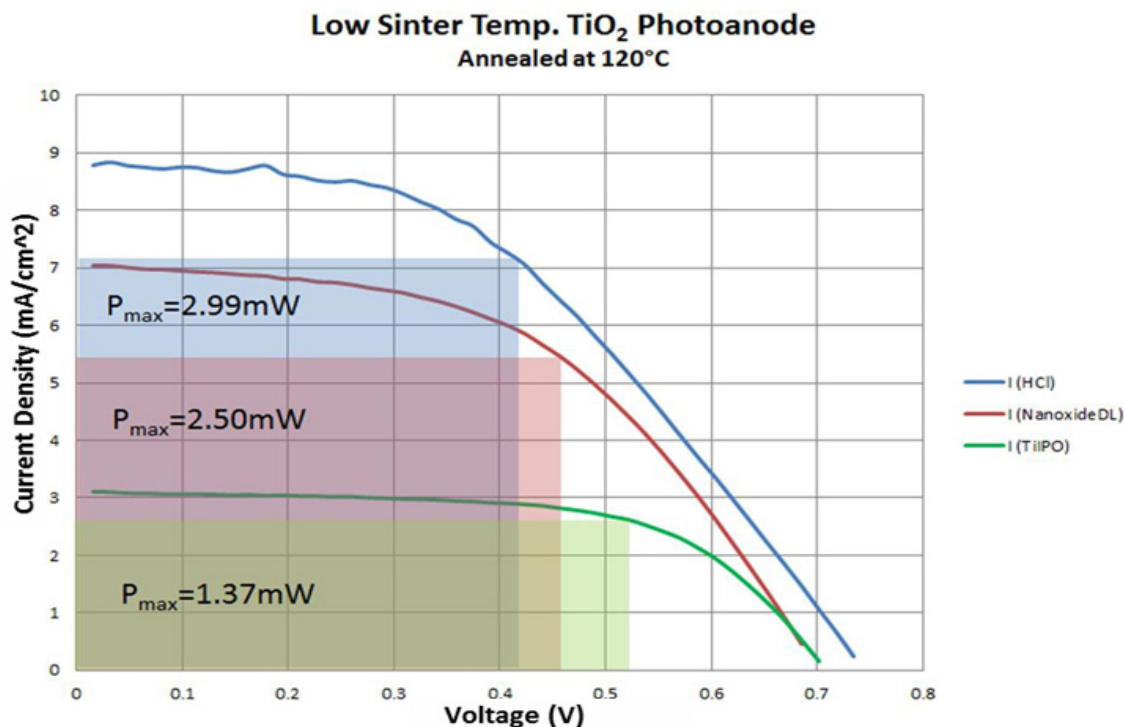


Figure 4. Current vs. voltage plot for the three different low-temperature sintering electrodes (prepared in a co-sensitizer dye mix and employing EL-HPE electrolyte). The area of the test cell photoanode for each device was  $1 \text{ cm}^2$ .

Next, the dyes used in the standard test cells were characterized with UV-Vis spectroscopy to determine their absorbance spectra. Approximately  $20 \mu\text{L}$  of the ethanol dye dispersion was pipetted onto a Nanodrop 2000 (Thermo Scientific); the normalized absorbance spectra can be seen in figure 5. The results of the UV-Vis spectroscopy reveal peaks for the ruthenium N719

dye at 315, 385, and 530 nm corresponding to electron transition energies of 3.94, 3.22, and 2.34 eV, respectively. The D149 dye has absorption maxima at 387 nm and 530 nm, similar to that of the Ru dye; however, the extinction coefficient for the D149 is nearly double that of the N719. The co-sensitizer dye, an equimolar mix of the two dyes, offered the broadest and highest absorbance of incident light, and thus was used as the optimal sensitization solution for the DSSC test cells. The higher absorbance allows for more photon energy to be harvested, given a thinner photoanode layer, which is desirable to reduce the diffusion path length of the critical triiodide molecular species throughout the mesopores back to the counter-electrode.

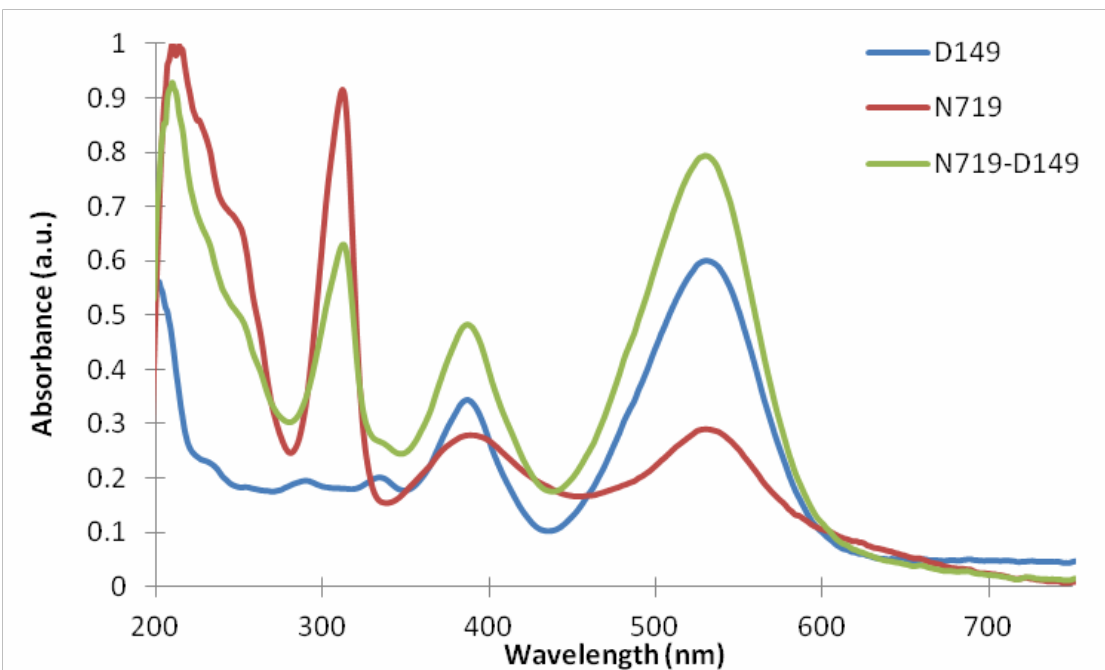


Figure 5. UV-Vis spectra of dyes D149, N719, and a 1:1 mixture.

To further elucidate the effectiveness of each dye type and mixture, test cells with each dye were constructed and tested for power and efficiency measurements. It is clear from the current-voltage plots in figure 6 that the combination of the N719 and D149 results in the highest current density and subsequently the most efficient device. It is likely that the broadened absorption spectra and intensity of the co-sensitizer dye mix results in more efficient and complete photon capture from the same thickness titania film. These results are consistent with the UV-Vis spectra of the dye solutions in the visible regions of the spectrum, where the combination of the two dyes results in a more intense and broad absorption spectra. Each dye tested was lacking in absorption of red to infrared photon energies; further research with quantum dot charge transfer complexes (3) may aid in capture of these wavelengths and further increase the efficiencies of DSSC modules.

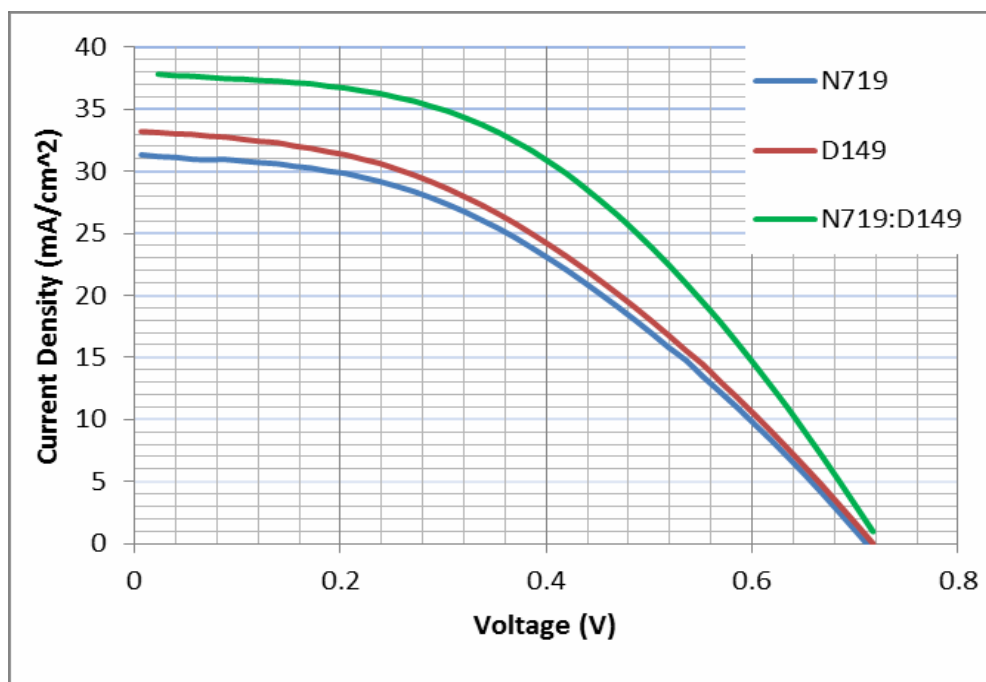


Figure 6. Current-voltage plots of DSSC test cells made with commercial Dyesol paste and dyes N719, D149, and an equimolar mix of the two.

Once a standard protocol for making consistent highly efficient test cells was developed, the commercial electrolyte EI-HPE was substituted for more stable RTIL electrolyte blends. The current-voltage plots for the high- and low-viscosity Z132 and B136, respectively, are shown in figure 7; the inscribed rectangles indicate the maximum power point on the characteristic I-V curve. The open cell voltages, short circuit current density, maximum power output, fill factor, and cell conversion efficiencies for the standard versus RTIL-based electrolytes are summarized in table 1.



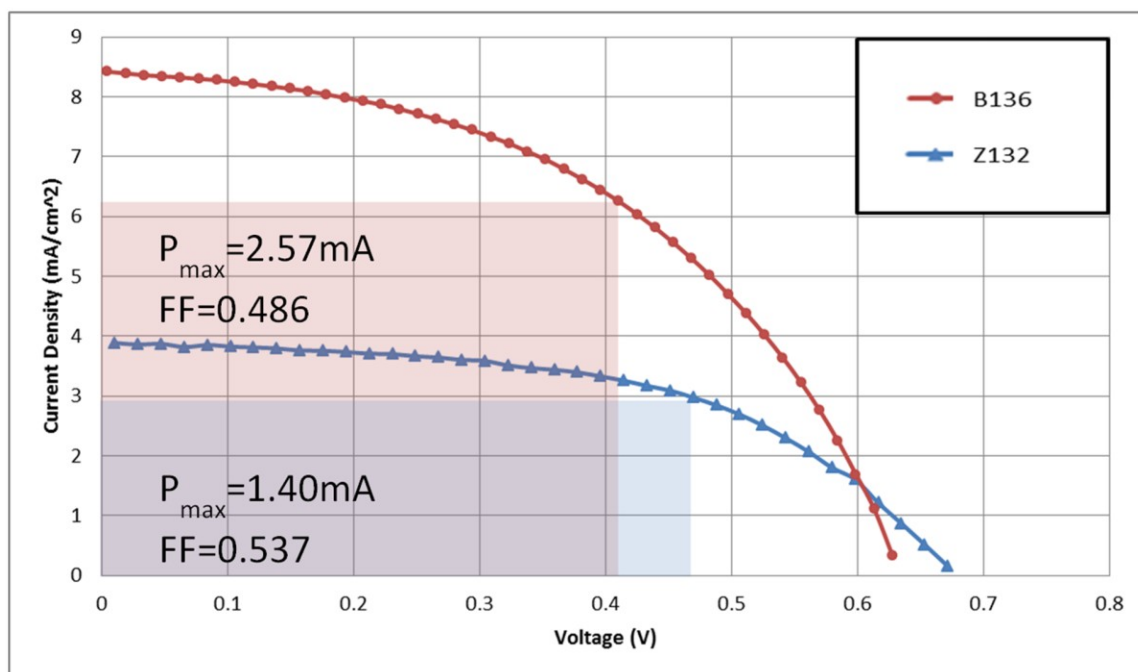


Figure 7. Current density vs. voltage plot for the nonvolatile RTIL electrolytes B136 (circle markers) and Z132 (triangle markers). Also shown is the max power rectangle inscribed and fill factor of the cells.

Table 1. Results of the tested electrolyte systems in standard test cells.

Electrolyte	$V_{oc}$ (mV)	$J_{sc}$ (mA cm <sup>-2</sup> )	$P_{max}$ (mW cm <sup>-2</sup> )	FF	$\eta$ (%)
EL-HPE	0.717	37.8	12.54	0.462	8.96
Z132	0.671	3.89	1.39	0.537	0.993
B136	0.628	8.42	2.57	0.486	1.84

It is clear from the plot in figure 7 that the lower viscosity electrolyte had a higher power conversion efficiency and current density compared to the more viscous Z132 electrolyte.

This is likely due to mass transport limitations of the bulky triiodide redox species and the resultant reduction in regeneration of oxidized dye molecules. Being able to minimize steric diffusion hindrances will be key to developing more advanced ionic liquid electrolytes for next generation DSSCs.

---

## 4. Summary and Conclusion

---

The recent shift towards renewable energy resources has fostered the development of novel photovoltaic technologies. In particular, robotic platforms running on limited electric power supplies stand to gain a much-extended runtime with on-the-go recharging capabilities. DSSCs are a new class of cheap, flexible, and efficient photovoltaic devices, well suited for incorporating onto the exterior of robotic vehicles. Electrolyte blends based on volatile organic compounds limit the practicality of these devices; however, nonvolatile ionic liquid electrolyte blends are capable of replacing their volatile organic solvent counterparts. High- and low-viscosity electrolytes based on imidazolium ionic liquids with a coupled iodide/triiodide redox pair were prepared and tested to determine their performance in optimized DSSC modules. The best performing electrolyte was found to be the lower viscosity blend, likely due to increased diffusion rates of the larger triiodide molecule back to the counter-electrode. In conclusion, future developments of RTIL electrolytes should focus on decreasing the viscosity of the blend while maintaining high electrical conductivity and electrochemical stability.

---

## 5. References

---

1. O'Regan, B.; Grätzel, M. A Low-Cost, High Efficiency Solar Cell Based on Dye\_Sensitized Colloidal TiO<sub>2</sub> Films. *Nature* **1991**, *353*, 737–740.
2. Snaith, H. J. The Perils of Solar Cell Efficiency Measurements. *Nature Photonics* **2012**, *6*, 337–340.
3. Cramer, H.; Dandekar, V.; Griep, M.; Karna, S.; Lee, E.; *Chemical vs. Sonochemical Synthesis and Characterization of Silver, Gold, and Hybrid Nanoparticles*; ARL-TR-5764; U.S. Army Research Laboratory: Aberdeen Proving Ground, MD, 2011. Also available at [http://www.arl.army.mil/www/default.cfm?technical\\_report=6237](http://www.arl.army.mil/www/default.cfm?technical_report=6237)
4. Bauerle, P.; Fischer, M.; Mishra, A. Metal-Free Organic Dyes for Dye-Sensitized Solar Cells: From Structure Property Relationships to Design Rules. *Angew. Chem. Int. Ed.* **2009**, *48*, 2474–2499.
5. Hagfeldt, A.; Boschloo, G.; Sun, L. C.; Kloo, L.; Pettersson, H. Dye-Sensitized Solar Cells. *Chem. Rev.* **2010**, *110*, 6595–6663.
6. Kloo, L.; Gorlov, M. Ionic Liquid Electrolyte for Dye-Sensitized Solar Cells. *RSC DaltonTrans.* **2008**, *20*, 2655–2666.
7. Zakeeruddin, S. M.; Wang, P.; Humphry-Baker, R.; Gratzel, M. A Binary Ionic Liquid Electrolyte to Achieve  $\geq 7\%$  Power Conversion Efficiencies in Dye-Sensitized Solar Cells. *Chem. Mater.* **2004**, *16*, 2694–2696.
8. Stathatos, E.; Chen, Y.; Dionysiou, D. Quasi-Solid-State Dye-Sensitized Solar Cells Employing Nanocrystalline TiO<sub>2</sub> Films Made at Low Temperature. *Solar Energy Materials & Solar Cells* **2008**, *92*, 1358–1365.
9. Ke, C.-R.; Ting, J. -M. Anatase TiO<sub>2</sub> Beads Having Ultra-Fast Electron Diffusion Rates for Use in Low Temperature Flexible Dye-Sensitized Solar Cells. *Journal of Power Sources* **2012**, *208*, 316–321.

1 DEFENSE TECHNICAL  
(PDF) INFORMATION CTR  
DTIC OCA

2 DIRECTOR  
(PDF) US ARMY RESEARCH LAB  
RDRL CIO LL  
IMAL HRA MAIL & RECORDS MGMT

1 GOVT PRINTG OFC  
(PDF) A MALHOTRA

24 DIR USARL  
(19 PDF, RDRL SED C  
5 HC) C LUNDGREN  
C XU  
RDRL SER  
P AMIRTHARAJ  
RDRL SER L  
M DUBEY  
M ERVIN  
B PIEKARSKI  
RDRL VT  
M VALCO  
RDRL VTM  
M BUNDY (1 HC, 1 PDF)  
D COLE  
A HALL  
D LE (1 HC, 1 PDF)  
L NATARAJ (1 HC, 1 PDF)  
C SWEENEY (1 HC, 1 PDF)  
RDRL WM  
S KARNA (1 HC, 1 PDF)  
RDRL WMM A  
M GRIEP  
D OBRIEN  
E WETZEL  
RDRL WMM E  
E NGO  
RDRL WMM G  
J SNYDER